JOURNAL OF MATERIALS SCIENCE 23 (1988) 2355–2360

Large magnetoresistivity of sputtered Al–(O or N)–Bi alloys

A. INOUE, K. MATSUZAKI, S. SHIRAKAWA*, T. MASUMOTO
The Research Institute for Iron, Steel and Other Metals, Tohoku University, Sendai 980, Japan

Application of the sputtering technique to $(Al_2O_3)_xBi_{100-x}$ and $(AlN)_xBi_{100-x}$ (x = 0 to 100%) has been found to result in the formation of a duplex material consisting of hexagonal bismuth particles dispersed finely and homogeneously in amorphous Al_xO_y and Al_xN_y matrices. The particle size and interparticle distance of the bismuth phase were about 5 to 140 nm and 5 to 35 nm. The duplex alloys have high electrical resistivities ranging from 1.82×10^3 to $3.16 \times 10^5\,\mu\Omega$ cm combined with a negative temperature-dependent resistivity of 148 to 342% of ϱ_{273}. Furthermore, all the Al–O–Bi and Al–N–Bi alloys have been found to exhibit a positive magnetoresistive change and the maximum value, $\Delta\varrho(H)$, at 4.2 K and 7.5 T reaches $5.85 \times 10^4\,\mu\Omega$ cm for $(Al\text{–}O)_{65.7}Bi_{34.3}$ and $1.99 \times 10^5\,\mu\Omega$ cm for $(Al\text{–}N)_{69.7}Bi_{30.3}$. The large magnetoresistivities are probably due to the unique sputtered structure consisting of metallic bismuth particles with a long mean free path of electrons embedded finely and homogeneously in amorphous Al_xO_y or Al_xN_y matrix, resulting in the large difference of the relaxation times (different mobilities) of electron carriers. It has thus been demonstrated that the oxide- or nitride-based composite materials exhibiting large magnetoresistivities, which cannot be achieved in metallic composite materials, are obtained by sputtering simultaneously Al_2O_3 or AlN and bismuth which is immiscible to aluminium.

1. Introduction

It has been reported very recently that the rapid quenching of immiscible-type alloys from the liquid or vapour state results in the formation of the duplex structure consisting of metallic particles embedded finely and homogeneously in crystalline metallic [1, 2] and semiconducting [3, 4] phases and amorphous metallic [5–7], oxide [8, 9] and nitride [9] phases. Furthermore, these duplex materials have been found to exhibit unique electrical resistive, magnetoresistive and superconductive properties [1–9]. Among these materials, it is particularly notable that (1) melt-quenched Ge–Sn and Ge–Pb alloys exhibit high electrical resistivities ($\simeq 10^4\,\mu\Omega$ cm at 250 K) combined with a large positive temperature dependence of about 70 to 90% in the range from 4.2 to 273 K [3], and (2) melt-quenched Ge–Pb–Bi–Sn alloys have an upper critical magnetic field (H_{c2}) of 15 T at 3.0 K and the H_{c2} value extrapolated to 0 K reaches as high as about 30 T [4]. Such unique and useful properties have been thought to result from the unique duplex structure in which the metallic phase dispersed by an immiscible phenomenon of the constituent elements has a lattice parameter nearly the same as that of pure metals and does not contain any other elements constructing the matrix. Accordingly, the duplex materials exhibit uniquely combined properties of dispersed pure metals and semiconductive or insulative matrix. From the dramatic effects of the dispersed structure on electrical properties described above, it is reasonable to expect that duplex materials consisting of bismuth metal dispersed homogeneously in electrically highly resistive materials such as oxide, nitride and semiconductor, etc., exhibit a large magnetoresistivity, because bismuth has the largest magnetoresistivity of the metallic materials [10]. The aim of this paper is to examine the microstructure, electrical resistivity and magnetoresistivity of sputtered Al–O–Bi and Al–N–Bi alloys and to investigate the possibility of whether or not a new material with a large magnetoresistivity is prepared on the basis of the concept described above.

2. Experimental procedure

Alloys with compositions of $(Al\text{–}O)_xBi_{100-x}$ (x = 0, 35.1, 65.7, 87.6 and 95.2%) and $(Al\text{–}N)_xBi_{100-x}$ (x = 29.3, 69.7 and 90.0%) were sputtered on a water-cooled ceramic substrate into a form of rectangular film with a thickness of 40 to 60 μm using a radio frequency (r.f.) sputtering apparatus. The Al–O–Bi and Al–N–Bi films for transmission electron microscopic (TEM) observation were sputtered on a rock salt substrate into a thin foil with a thickness of about 100 nm. The target cathode consisted of pure bismuth (99.99 wt %) and highly pure Al_2O_3 or AlN and the composition was controlled by changing the surface area ratio of the two constituent raw materials. After evacuating the sputtering chamber mounted with the target material up to 2×10^{-5} Pa, argon gas of 4 Pa was fed through an automatic gas-flow controller to make argon-plasma in the chamber.

**Permanent address*: Research and Development, Tanaka Denshi Kogyo Ltd, Mitaka 181, Japan.

0022–2461/88 $03.00 + .12 © *1988 Chapman and Hall Ltd.*

The argon-plasma was generated between a tungsten filament cathode and a stainless steel anode. The anode current usually supplied was 60 mA and the anode voltage was 1 kV. Prior to sputtering the target the substrate was sputtered to clean its surface for 5 min by applying a negative bias against the substrate. The gap between the target and substrate was fixed at 20 mm.

The structure of the sputtered films was examined by X-ray diffractometry and TEM. Measurement of electrical resistivity as a function of temperature and magnetic field was done using a conventional four-probe technique. A magnetic field up to 8 T was applied transversely to the specimen surface and the excited current. The temperature was measured using a calibrated germanium thermometer at temperatures below 90 K and a calibrated diode thermometer in the higher temperature range with an accuracy better than ± 0.01 and ± 0.1 K below and above 90 K, respectively.

3. Results

3.1. Sputtered structure

Fig. 1 shows the X-ray diffraction patterns of sputtered $(Al\text{-}O)_x Pb_{100-x}$ (x = 0, 35.1, 65.7 and 95.2%) films. All the patterns can only be identified as hexagonal bismuth; no diffraction peaks corresponding to Al_xO_y oxide are seen. It is thus notable that the diffraction peaks consist only of bismuth phase even for the Al-O-rich film containing 4.8% Bi. Although the intensity of bismuth diffraction peaks tends to decrease with decreasing bismuth content, there is no systematic variation in the peak position of bismuth phase with area ratio of bismuth to Al_2O_3. Additionally, one can notice that the number of diffraction peaks increases significantly with the coexistence of Al_xO_y phase. The change is thought to result from the increase in the randomness of crystal orientation for the bismuth phase embedded in the Al_xO_y phase. A similar X-ray diffraction pattern consisting only of hexagonal bismuth phase was also obtained for sputtered $(Al\text{-}N)_x Bi_{100-x}$ (x = 29.3, 69.7 and 90.0%) films.

In order to obtain information on the microstructure and crystal structure of Al_xO_y and Al_xN_y phases, as well as the dispersion state of the bismuth phase in sputtered Al-O-Bi and Al-N-Bi films, TEM observation was carried out for deposited $(Al\text{-}O)_x Bi_{100-x}$ (x = 35.1, 65.7 and 95.2%) and $(Al\text{-}N)_x Bi_{100-x}$ (x = 29.3, 69.7 and 90.0%) thin films. Figs 2 and 3 show bright-field electron micrographs and selected-area diffraction patterns of sputtered Al-O-Bi and Al-N-Bi films, respectively. The diffraction patterns revealed the coexistence of amorphous Al-O or Al-N and hexagonal bismuth phases for the Al-O- and Al-N-rich films. With decreasing x content, the broad diffraction peaks corresponding to an amorphous phase disappear and the patterns consist only of hexagonal bismuth phase. From the distinct appearance of amorphous halo rings for the Al-O- and Al-N-rich films, it is reasonably considered that the sputtered structure consists of amorphous Al_xO_y and hexagonal bismuth phases for $(Al\text{-}O)_x Bi_{100-x}$ films and amorphous Al_xN_y and hexagonal bismuth phases for

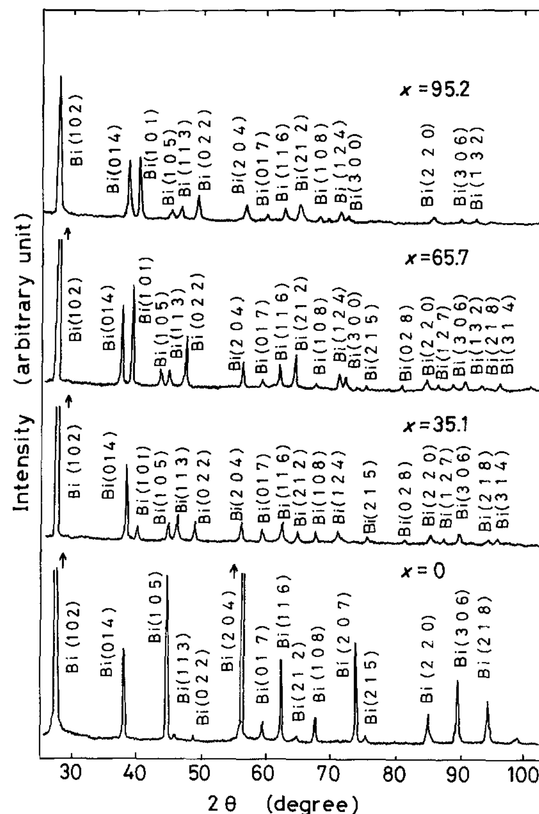

Figure 1 X-ray diffraction patterns of $(Al\text{-}O)_x Bi_{100-x}$ (x = 0, 35.1, 65.7 and 95.2%) sputtered films.

$(Al\text{-}N)_x Bi_{100-x}$ films. As shown in the bright-field images in Figs 2 and 3, the average particle size and interparticle spacing of bismuth phase tend to increase with increasing bismuth content from about 10 to 65 nm and 5 to 35 nm, respectively, for $(Al\text{-}O)_x Bi_{100-x}$ films and from about 5 to 140 nm and 5 to 30 nm, respectively, for $(Al\text{-}N)_x Bi_{100-x}$ films. The $(Al\text{-}O)_x Bi_{100-x}$ and $(Al\text{-}N)_x Bi_{100-x}$ films are concluded to have the duplex structure consisting of fine hexagonal bismuth particles embedded homogeneously in the amorphous phase of Al_xO_y and Al_xN_y. Fig. 4 shows the change in the lattice parameter of bismuth in $(Al\text{-}O)_x Bi_{100-x}$ and $(Al\text{-}N)_x Bi_{100-x}$ films determined from the X-ray diffraction data with area ratio of bismuth to Al_2O_3 or AlN in the target. The lattice parameter for both the alloy systems remains constant (a = 0.456 nm and c = 1.187 nm) over the whole composition range and agrees with that (a = 0.454 59 nm and c = 1.186 22 nm) [11] of pure bismuth. Therefore, it is concluded that detectable dissolution of aluminium, oxygen and/or nitrogen into the bismuth phase does not take place even for the Al_xO_y- and Al_xN_y-rich films containing about 5% Bi, in accordance with the expectation from Al-Bi equilibrium phase diagram [12].

3.2. Electrical resistivity

Fig. 5 plots the electrical resistivity at 4.2 and 273 K for sputtered $(Al\text{-}O)_x Bi_{100-x}$ and $(Al\text{-}N)_x Bi_{100-x}$ films as a function of area ratio of Al_2O_3 or AlN to bismuth in the target. The resistivity at 4.2 K is $6.61 \times 10^3\ \mu\Omega$ cm for the bismuth film, increases gradually with increasing area fraction of Al_2O_3 or AlN and reaches $3.98 \times 10^4\ \mu\Omega$ cm for $(Al\text{-}O)_{95.2} Bi_{4.8}$ and

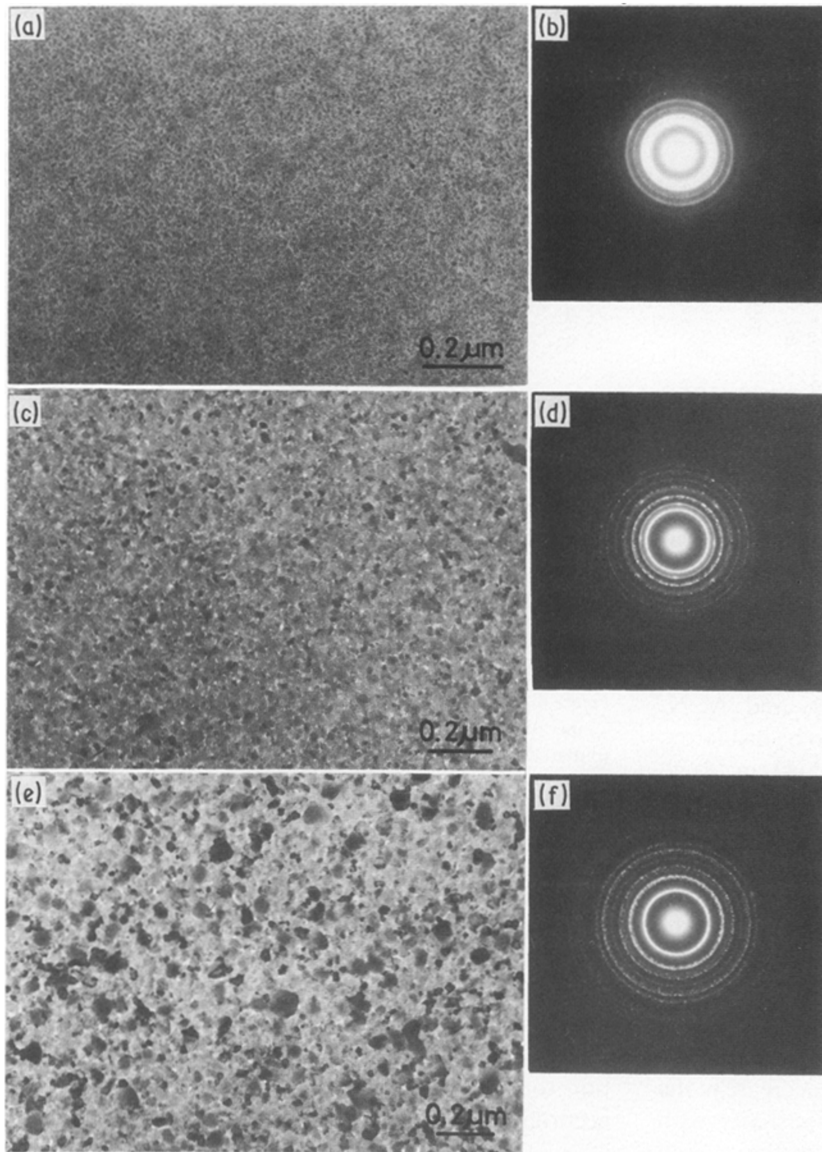

Figure 2 Bright-field electron micrographs and selected-area diffraction patterns of $(\text{Al–O})_x\text{Bi}_{100-x}$ sputtered films. (a, b) $x = 35.1\%$; (c, d) $x = 65.7\%$; (e, f) $x = 95.2\%$.

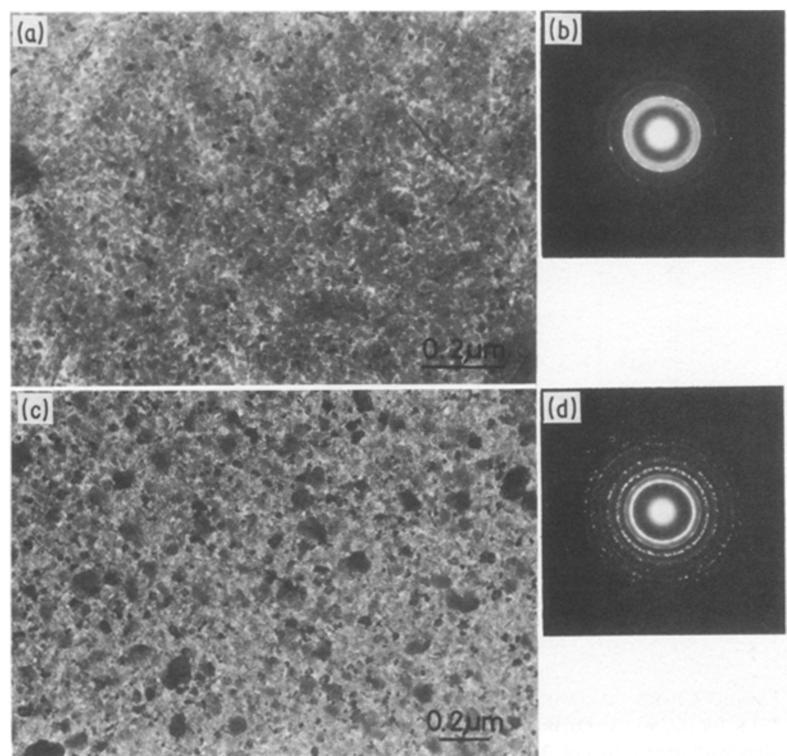

Figure 3 Bright-field electron micrographs and selected-area diffraction patterns of $(\text{Al–N})_x\text{Bi}_{100-x}$ sputtered films. (a, b) $x = 29.3\%$; (c, d) $x = 69.7\%$.

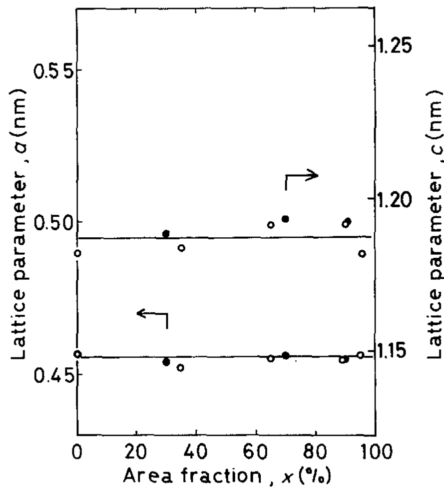

Figure 4 Change in the lattice parameter of hexagonal bismuth in (○) $(Al–O)_xBi_{100-x}$ and (●) $(Al–N)_xBi_{100-x}$ sputtered films with area ratios of Al_2O_3 or AlN in the target.

$2.40 \times 10^6\ \mu\Omega$cm for $(Al–N)_{95.0}Bi_{5.0}$. A similar compositional dependence of resistivity is also seen for the values at 273 K. The sputtered Al_xO_y and Al_xN_y amorphous films have been confirmed to be insulators with an ultrahigh resistivity above $10^9\ \mu\Omega$cm [8, 9]. The normalized electrical resistant curves (R/R_{273}) as a function of temperature are shown in Fig. 6 for $(Al–O)_xBi_{100-x}$ (x = 0, 35.1, 65.7, 87.6 and 95.2%) and in Fig. 7 for $(Al–N)_xBi_{100-x}$ (x = 29.3, 69.7 and 90.0%). The electrical resistivity of all the Al–O–Bi and Al–N–Bi alloys shows a negative temperature dependence and decreases significantly with increasing temperature from 4.2 to 273 K, e.g. 3.98×10^4 to $2.37 \times 10^4\ \mu\Omega$cm for $(Al–O)_{95.2}Bi_{4.8}$ and 2.40×10^6 to $3.16 \times 10^5\ \mu\Omega$cm for $(Al–N)_{90}Bi_{10}$. The decrease in the negative temperature dependence of resistivity with increasing Al_xO_y content is in contrast to the general tendency that the increase in resistivity results in an increase in the slope of the negative temperature dependence and the reason for such an unexpected tendency remains unknown.

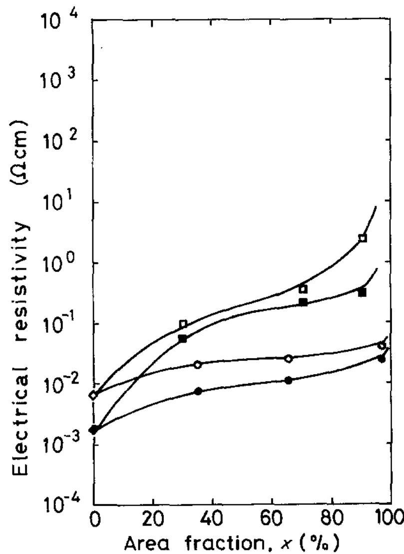

Figure 5 Change in electrical resistivity at (○, □) 4.2 and (●, ■) 273 K for (○, ●) $(Al–O)_xBi_{100-x}$ and (□, ■) $(Al–N)_xBi_{100-x}$ sputtered films with area ratios of Al_2O_3 or AlN in the target.

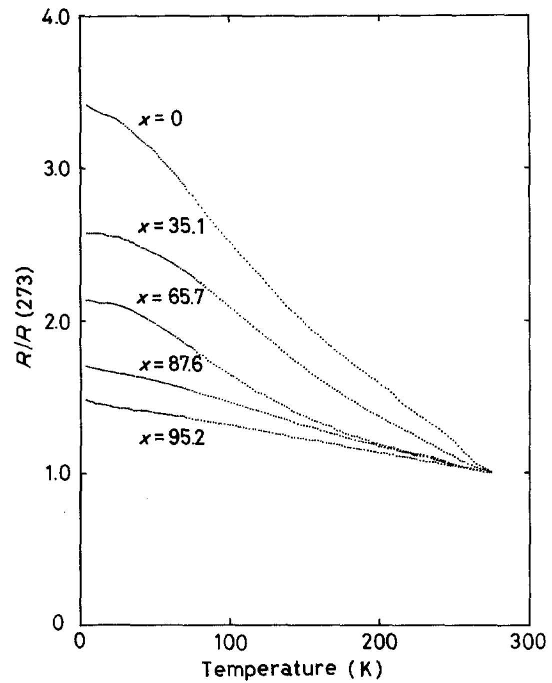

Figure 6 Normalized electrical resistance, R/R_{273}, as a function of temperature for $(Al–O)_xBi_{100-x}$ (x = 0, 35.1, 65.7, 87.6 and 95.2%) sputtered films.

3.3. Magnetoresistivity

Figs 8 and 9 show the change in electrical resistivity at 4.2 K as a function of transversely applied magnetic field for sputtered $(Al–O)_xBi_{100-x}$ (x = 0, 35.1, 65.7, 87.6 and 95.0%) and $(Al–N)_xBi_{100-x}$ (x = 29.3, 69.7 and 90.0%) films. It can be seen that the transverse magnetoresistivities ($\Delta\varrho/\varrho$) of all the alloys are positive and increase with increasing magnetic field in proportion to H^n with n ranging from about 0.5 to 1.0, in accordance with the tendency [13] for a number of

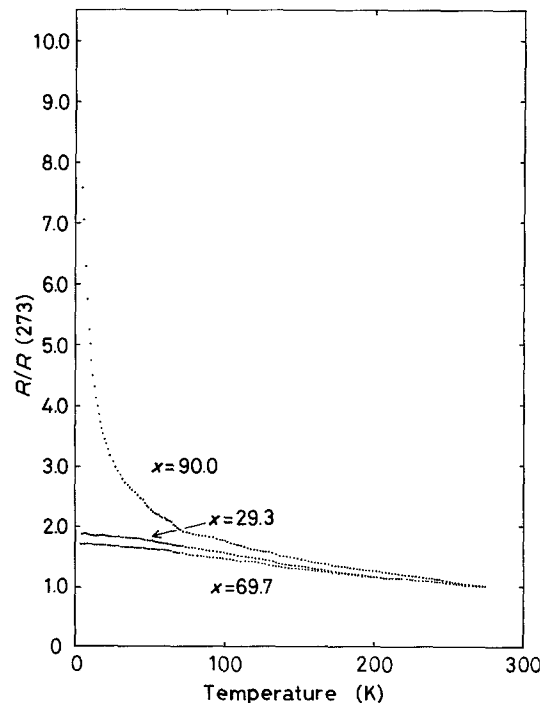

Figure 7 Normalized electrical resistance, R/R_{273}, as a function of temperature for $(Al–N)_xBi_{100-x}$ (x = 29.3, 69.7 and 90.0%) sputtered films.

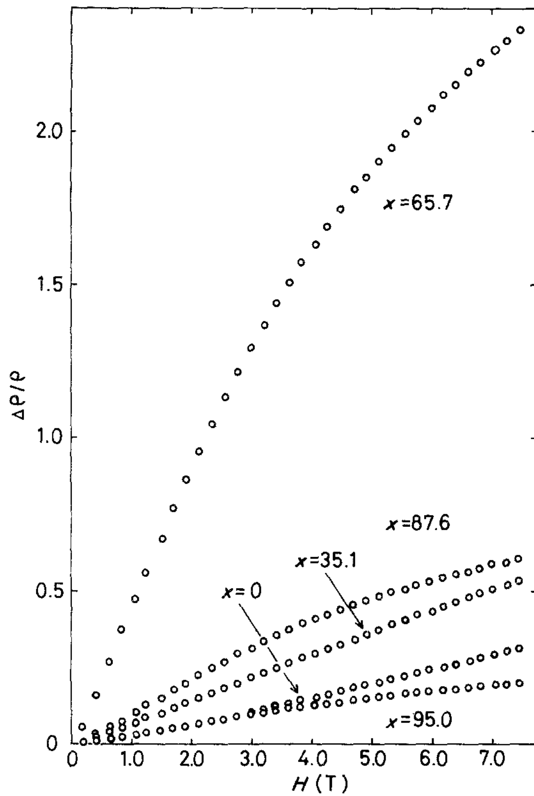

Figure 8 Magnetoresistivity $\Delta\varrho/\varrho$ at 4.2 K as a function of applied field for $(Al–O)_x Bi_{100-x}$ (x = 0, 35.1, 65.7, 87.6 and 95.0%) sputtered films.

metals and alloys. Fig. 10 shows the change in the $\Delta\varrho/\varrho$ values of $(Al–O)_x Bi_{100-x}$ and $(Al–N)_x Bi_{100-x}$ films under an applied field of 7.5 T at 4.2 K with the area fraction of Al_2O_3 or AlN to bismuth in the target, together with the data of sputtered $Ge_x Bi_{100-x}$ and $Si_x Bi_{100-x}$ films measured under the same conditions. The four alloys exhibit a similar compositional dependence and $\Delta\varrho/\varrho$ has a maximum value at a certain area

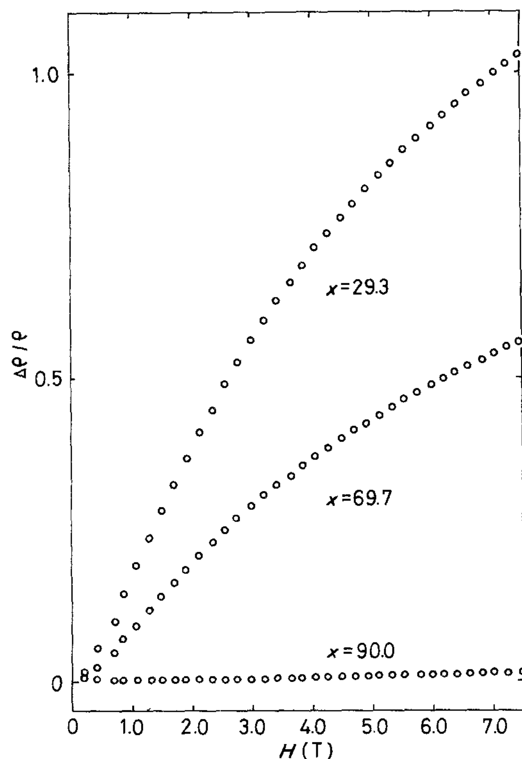

Figure 9 Magnetoresistivity $\Delta\varrho/\varrho$ at 4.2 K as a function of applied field for $(Al–N)_x Bi_{100-x}$ (x = 29.3, 69.7 and 90.0%) sputtered films.

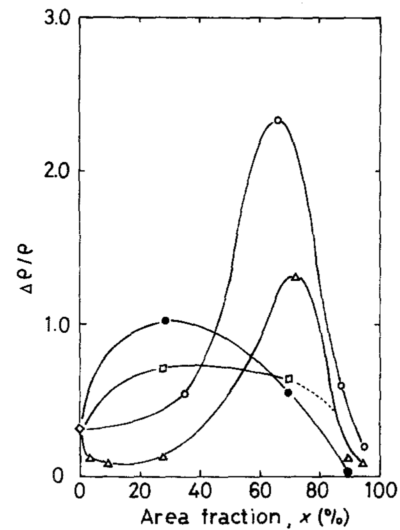

Figure 10 Change in magnetoresistivity $\Delta\varrho/\varrho$ at 4.2 K and 7.5 T for (○) $(Al–O)_x Bi_{100-x}$ and (●) $(Al–N)_x Bi_{100-x}$ sputtered films with area ratio of Al_2O_3 or AlN in target. The data of (△) $Ge_x Bi_{100-x}$ and (□) $Si_x Bi_{100-x}$ sputtered films with amorphous germanium or silicon and hexagonal bismuth phases are also shown for comparison.

fraction. However, the area fraction at which $\Delta\varrho/\varrho$ shows a maximum value is different between the Al–O–Bi or Ge–Bi alloys and the Al–N–Bi or Si–Bi alloys, being 0.65 to 0.70 for the former alloys and 0.25 to 0.30 for the latter alloys. It is particularly notable that the magnetoresistive change at 7.5 T is as large as 233% for $(Al–O)_{65.7}Bi_{34.3}$, 130% for $Ge_{70}Bi_{30}$, 103% for $(Al–N)_{29.3}Bi_{70.7}$ and 71% for $Si_{28}Bi_{72}$. Furthermore, as shown in Fig. 11, the magnetoresistive increment increases with increasing x content, reaches as much as $5.85 \times 10^4\,\mu\Omega$cm for $(Al–O)_{65.7}Bi_{34.3}$ and $1.99 \times 10^5\,\mu\Omega$cm for $(Al–N)_{69.7}Bi_{30.3}$, and tends to decrease with further increasing x content. The large resistive increments by magnetoresistivity indicate that the Al–O–Bi and Al–N–Bi films can measure very sensitively the change in resistivity with applied field, even for the short sample.

4. Discussion

It was shown in Section 3 that the sputtered Al–O–Bi and Al–N–Bi alloys consist of the fine duplex structure

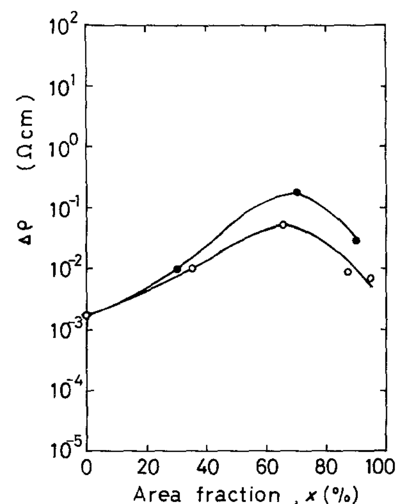

Figure 11 Change in the resistive increment by magnetoresistivity at 4.2 K and 7.5 T for (○) $(Al–O)_x Bi_{100-x}$ and (●) $(Al–N)_x Bi_{100-x}$ sputtered films with area ratios of Al_2O_3 or AlN in the target.

consisting of Al–O or Al–N and bismuth phases and the electrical resistive behaviour results mainly from the conduction electrons localized in the bismuth phase. It is known that the magnetoresistance is strongly dependent on the mean free path of electrons and relaxation times (different mobilities) of electron carriers and the longer the mean free path and the larger the difference of the relaxation times, the larger is the magnitude of the magnetoresistance. It was shown that the metallic bismuth phase embedded in the germanium phase does not dissolve an appreciable amount of aluminium, oxygen or nitrogen and is regarded as a pure metal with a long mean free path of electrons. Accordingly, the Al–O–Bi and Al–N–Bi duplex alloys are expected to exhibit a magnetoresistance larger than that of pure bismuth metal.

Kohler [14] indicates that the reduced magnetoresistivity, $\Delta\varrho/\varrho$, where ϱ is the zero-field resistivity and $\Delta\varrho$ the increase due to the field H, is a function of the ratio H/ϱ:

$$\Delta\varrho/\varrho = f(H/\varrho) \quad (5)$$

Fig. 12 shows the so-called reduced Kohler plot [15] in which the transverse magnetoresistivities $\Delta\varrho/\varrho$ of sputtered $(Al\text{–}O)_{65.7}Bi_{34.3}$, $(Al\text{–}N)_{29.3}Bi_{70.7}$, $(Al\text{–}N)_{69.7}Bi_{38.3}$ and bismuth films are presented as a function of the ratio $H\varrho_\theta/\varrho$ based on the data shown in Figs 8 and 9. Here ϱ_θ is the resistivity at $T = \theta_D$ K. It can be seen that $\Delta\varrho/\varrho$ of the Al–O–Bi and Al–N–Bi alloys increases almost linearly with increasing $H\varrho_\theta/\varrho$, in good agreement with the tendency for sputtered bismuth metal. This agreement allows us to infer that the generation of magnetoresistance for the Al–O–Bi and Al–N–Bi alloys is attributed to the bismuth metal embedded in Al–O and Al–N amorphous matrices. However, the values in the $\Delta\varrho/\varrho\text{–}H\varrho_\theta/\varrho$ relation for the Al–O–Bi and Al–N–Bi alloys deviate from those of sputtered bismuth metal and lie at the higher side of

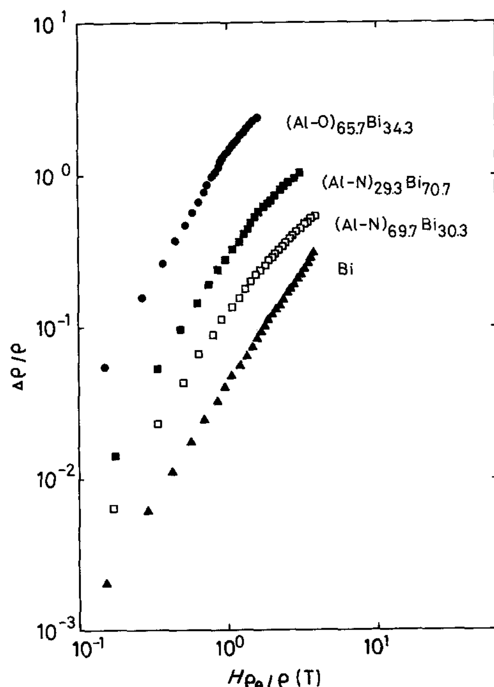

Figure 12 Transverese magnetoresistivity of $(Al\text{–}O)_xBi_{100-x}$, $(Al\text{–}N)_xBi_{100-x}$ and bismuth sputtered films plotted on a reduced Kohler diagram.

$\Delta\varrho/\varrho$ and at the lower side of $H\varrho_\theta/\varrho$. This suggests that the large magnetoresistance for the Al–O–Bi and Al–N–Bi alloys results from the large field dependence of the mean free path of electrons for metallic bismuth itself, and the increase in the ease of the breaking-off of the conducting path caused by the isolated dispersion of bismuth metal in Al–O and Al–N amorphous matrices. A more systematic investigation of the magnetoresistivities of oxide–metal, nitride–metal and semiconductor–metal duplex materials, which is presently being carried out, is expected to shed some light on clarification of the mechanism of the enhanced magnetoresistivity for Al–O–Bi and Al–N–Bi alloys.

5. Conclusion

The magnetoresistivity at 4.2 K for $(Al\text{–}O)_xBi_{100-x}$ and $(Al\text{–}N)_xBi_{100-x}$ films is positive and increases with H^n ($n = 0.5$ to 1). The magnetoresistive change at 7.5 T is as large as 233% ($5.85 \times 10^4\,\mu\Omega$ cm) for $(Al\text{–}O)_{65.7}Bi_{34.3}$ and 103% ($9.84 \times 10^4\,\mu\Omega$ cm) for $(Al\text{–}N)_{29.3}Bi_{70.7}$, being much larger than that (31%, $\simeq 2.05 \times 10^3\,\mu\Omega$ cm) for sputtered bismuth metal. The markedly enhanced magnetoresistivity is thought to be due to the fine and homogeneous dispersion of hexagonal bismuth metal with a long mean free path of electrons in Al_xO_y or Al_xN_y matrix and the resultant large difference in the relaxation times of electron carriers. It is thus very important from the scientific and engineering points of view that the duplex alloys consisting of fine metallic bismuth particles dispersed in Al_xO_y and Al_xN_y matrices can be prepared by co-sputtering Al_2O_3 or AlN and bismuth by taking advantage of the immiscible phenomenon between aluminium and bismuth elements, and that these duplex alloys exhibit large magnetoresistivities.

References

1. A. INOUE, N. YANO, K. MATSUZAKI and T. MASUMOTO, *J. Mater. Sci.* **22** (1987) 123.
2. *Idem, ibid.* **22** (1987) 1827.
3. *Idem, Int. J. Rapid Solidification* **2** (1986) 175.
4. K. MATSUZAKI, A. INOUE, M. OGUCHI and T. MASUMOTO, *ibid.* **3** (1987) 1.
5. A. INOUE, M. OGUCHI, K. MATSUZAKI and T. MASUMOTO, *ibid.* **1** (1984–85) 273.
6. A. INOUE, M. OGUCHI, K. MATSUZAKI, Y. HARAKAWA and T. MASUMOTO, *J. Mater. Sci.* **21** (1986) 260.
7. K. MATSUZAKI, A. INOUE, M. OGUCHI, N. TOYOTA and T. MASUMOTO, *Int. J. Rapid Solidification* **2** (1987) 231.
8. A. INOUE, T. OGASHIWA, K. MATSUZAKI and T. MASUMOTO, *J. Mater. Sci.* **22** (1987) 2063.
9. A. INOUE, K. MATSUZAKI, S. SHIRAKAWA and T. MASUMOTO, *J. Mater. Sci.* in press.
10. G. T. MEADEN, "Electrical Resistance of Metals", (Heywood Books, London, 1966) p. 132.
11. W. B. PEARSON, "Handbook of Lattice Spacings and Structures of Metals and Alloys" (Pergamon Press, London, 1958) p. 124.
12. M. HANSEN, "Constitution of Binary Alloys" (McGraw-Hill, New York, 1958) p. 74.
13. M. KOHLER, *Ann. Physik* **32** (1938) 211.
14. *Idem, ibid.* **6** (1949) 18.
15. E. JUSTI, *Phys. Z.* **41** (1940) 486, 563.

Received 2 February and accepted 15 April 1987